

Distribution of ^{230}Th in the Labrador Sea and its relation to ventilation

S.B. Moran ^{a,*}, M.A. Charette ^a, J.A. Hoff ^b, R.L. Edwards ^b, W.M. Landing ^c

^a Graduate School of Oceanography, University of Rhode Island, Narragansett, RI 02882-1197, USA

^b Department of Geology and Geophysics, University of Minnesota, Minneapolis, MN 55455, USA

^c Department of Oceanography, Florida State University, Tallahassee, FL 32306, USA

Received 21 June 1996; accepted 25 April 1997

Abstract

Measurements of dissolved and particulate ^{230}Th and ^{232}Th by thermal ionization mass spectrometry were made on samples collected from the Labrador Sea and the Denmark Strait and Iceland–Scotland overflow waters. The large-scale feature of low and invariant ^{230}Th evident in deep waters of the Labrador Sea and previously observed in the deep northern Atlantic can be reproduced using a reversible scavenging model that includes the effect of ventilation. Advective transport also must be important in the redistribution of ^{230}Th in other regions of the Atlantic and for other long-lived tracers, such as ^{231}Pa , ^{26}Al and ^{10}Be . © 1997 Elsevier Science B.V.

Keywords: Labrador Sea; thorium

1. Introduction

The production and southward transport of North Atlantic Deep Water (NADW) plays a key role in the oceanic heat budget, carbon and nutrient cycles, and global climate. New insights into the mode of deep water circulation in the Atlantic have been derived from sediment studies of the particle-reactive radionuclides ^{230}Th ($t_{1/2} = 7.5 \times 10^4$ yr) and ^{231}Pa ($t_{1/2} = 3.2 \times 10^4$ yr) [1], produced in situ from dissolved ^{238}U and ^{235}U , respectively. In contrast to the Pacific [2–5], the importance of horizontal advection in redistributing these long-lived tracers is indicated by the relatively low excess sediment $^{231}\text{Pa}/^{230}\text{Th}$

ratios in the interior basins and ocean margins in the Atlantic [1]. Yu et al. [1] estimated that ~10% of the ^{230}Th and ~45% of the ^{231}Pa produced in the Atlantic is transported southwards by advection.

Water column distributions of ^{230}Th and ^{231}Pa in the contemporary Atlantic provide an important constraint on the advective transport of these tracers and hence their use as a proxy for past changes in deep water circulation. There are, however, only a few published profiles of ^{230}Th from the Atlantic, and fewer still for ^{231}Pa . In the eastern central Atlantic the ^{230}Th profile is characterized by low values that increase with depth [6]. Cochran et al. [7] reported the only full depth profiles of ^{230}Th in the western North Atlantic at the Nares and Hatteras Abyssal Plains. A key feature of their profiles is the relatively low and invariant ^{230}Th concentrations in the deep

* Corresponding author. Tel.: +1 401 874 6530. Fax: +1 401 874 6811. E-mail: moran@gsosun1.gso.uri.edu

waters. They suggested that the low and nearly constant ^{230}Th activities in the deep Northwest Atlantic were due to southward flowing NADW containing low ^{230}Th . In fact, low ^{230}Th has recently been reported in the deep Norwegian Sea and Denmark Strait overflow waters [11]. This is in contrast to profiles in the western North Pacific [8], which are characterized by an approximately linear increase with depth and ~ 2 -fold higher ^{230}Th concentrations. In the South Atlantic, ^{230}Th exhibits a similar distribution, though with higher values in these older deep waters [9]. For ^{231}Pa , profiles from the North Atlantic [10] and South Atlantic [9] are similar and indicate relatively constant values below ~ 1000 m.

In this study, ^{230}Th results from the Labrador Sea and NADW overflow waters are combined with a scavenging–mixing model [9] to quantify the large-scale effect of scavenging and water mass age on ^{230}Th distributions in the Atlantic. The implication is that advective transport is important in controlling ^{230}Th in the deep north Atlantic. Moreover, similar considerations must apply in other regions of the Atlantic and to other long-lived tracers, such as ^{231}Pa , ^{26}Al and ^{10}Be .

2. Methods

2.1. Sampling and TIMS Th analysis

Seawater samples were collected from the Labrador Sea (Stn. 2), Denmark Strait (Stn. 12), and the Faeroe Bank Channel (Stn. 14) during the IOC-93 expedition in August, 1993 (Fig. 1). Also indicated in Fig. 1 are Stn. 13 and Stn. 7, for which ^{230}Th and ^{232}Th results were recently reported [11]. Sampling was conducted using established clean techniques to minimize sources of contamination, which could result in significant ^{230}Th and ^{232}Th blanks due to the small sample sizes used in the study. Samples were collected using 12 l and 30 l Go-Flo bottles modified for trace metal sampling and deployed on a Kevlar hydrowire. Seawater was filtered directly from the Go-Flo bottles using N_2 over-pressure through acid-cleaned, $0.4\ \mu\text{m}$, 142 mm diameter, Nuclepore filters held in teflon filter holders. Filtered and unfiltered samples (1–2 l) were acidified to pH 2 using concentrated Seastar HCl and stored for later analy-

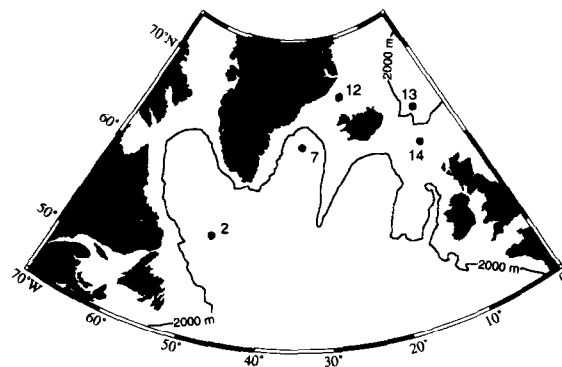


Fig. 1. Map showing the IOC-93 stations in the Labrador Sea (Stn. 2), northern Denmark Strait (Stn. 12), and the Faeroe Bank Channel (Stn. 14). ^{230}Th and ^{232}Th results have been reported [11] for the southern Denmark Strait (Stn. 7) and Norwegian Sea (Stn. 13).

sis. Nuclepore filters containing suspended particulate matter filtered from 14–22 l were rinsed with Milli-Q water (pH 8) to remove salts, folded, and stored frozen in plastic bags until further processing in the shore-based laboratory. All sample manipulations at sea were conducted in a laminar-flow bench.

Separation and purification of Th was performed in clean rooms at the Minnesota Isotope Lab (MIL) using ultrapure reagents [12,13]. A method for determination of ^{231}Pa in these samples using TIMS was not developed when these analyses were conducted, although this is now feasible [14]. Samples were weighed and spiked with ~ 50 pg of ^{229}Th tracer and ~ 6 mg of Fe carrier. After allowing the spike to equilibrate with the sample for at least 5 days, Th was co-precipitated using FeOH_3 by addition of NH_4OH (pH 8). The precipitate was collected by centrifugation and dissolved in 7 M HNO_3 . Th was purified by passing the solution through a teflon micro-column containing 0.6 ml of anion-exchange resin (BioRad AG 1-X8, 100–200 mesh) that was conditioned using several column volumes (CV) of 7 M HNO_3 . Samples were added to the column in 0.6 ml (1 CV) of 7 M HNO_3 , washed with ~ 1 ml (1.5 CV) of 7 M HNO_3 , and Th eluted using 1.8 ml (3 CV) of 6 M HCl. Th was further purified in a similar manner using a second column containing 0.15 ml of AG 1-X8 resin. The final Th eluant was evaporated to dryness and converted to nitrate form for loading in the mass spectrometer. For the particu-

late samples, the Nuclepore filters, ^{229}Th tracer, and 20 ml of concentrated $\text{HCl-HNO}_3\text{-HF}$ were added to teflon bombs and digested in a microwave oven for 12 h [15]. Th was purified in the resulting solution using the procedures described above.

Analyses were performed at MIL using a Finnigan MAT 262 RPQ mass spectrometer operating in pulse counting mode. Samples were loaded in dilute HNO_3 and dried on zone-refined Re filaments that had been previously checked for contamination in the Th mass range. The samples were then covered with colloidal graphite and further evaporated to dryness. Data were collected at temperatures between 1750°C and 1950°C by magnet controlled peak switching between ^{229}Th , ^{230}Th , and ^{232}Th . Beam intensities on ^{230}Th were typically 1–3 counts per second. Corrections for blanks, dark noise, and abundance sensitivity were made off-line. The blank contribution from Fe co-precipitation and anion-exchange separation was determined from 4 blank runs to be 0.1 ± 0.1 fg for ^{230}Th ($1.7 \pm 1.8\%$ of ^{230}Th analyzed) and 3.3 ± 1.5 pg for ^{232}Th ($5.6 \pm 5.5\%$ of ^{232}Th analyzed). Blanks for the filter digestion procedures and anion-exchange purification were determined from 2 blank runs to be 0.3 ± 0.1 fg for ^{230}Th ($5.3 \pm 4.3\%$ of ^{230}Th analyzed) and 25 ± 10 pg for ^{232}Th ($12.5 \pm 6.8\%$ of ^{232}Th analyzed).

2.2. Ancillary analyses

Salinity and temperature data were obtained using a calibrated CTD. Salinities were also determined using a Guildline Autosol salinometer on each Go-flo bottle from which Th samples were drawn. Dissolved Si was determined using standard colorimetric procedures and dissolved oxygen was analyzed by Winkler titration. Carbon tetrachloride was determined at sea using electron capture detection–gas chromatography.

3. Results

3.1. Hydrography

Hydrographic characteristics of the Labrador Sea at Stn. 2 are illustrated in depth profiles of dissolved oxygen, potential temperature, salinity, silicate, and carbon tetrachloride (Fig. 2a,b). The surface mixed layer is characterized by warm, low salinity, nutrient depleted water that shows no indication of the cold, low salinity water associated with the Labrador Current. Below the surface mixed layer, a subsurface minimum in dissolved oxygen is evident at 250 m, coincident with elevated Si concentrations. The almost uniform θ -S layer between 400 and 1900 m shows characteristics of Labrador Sea Water (LSW),

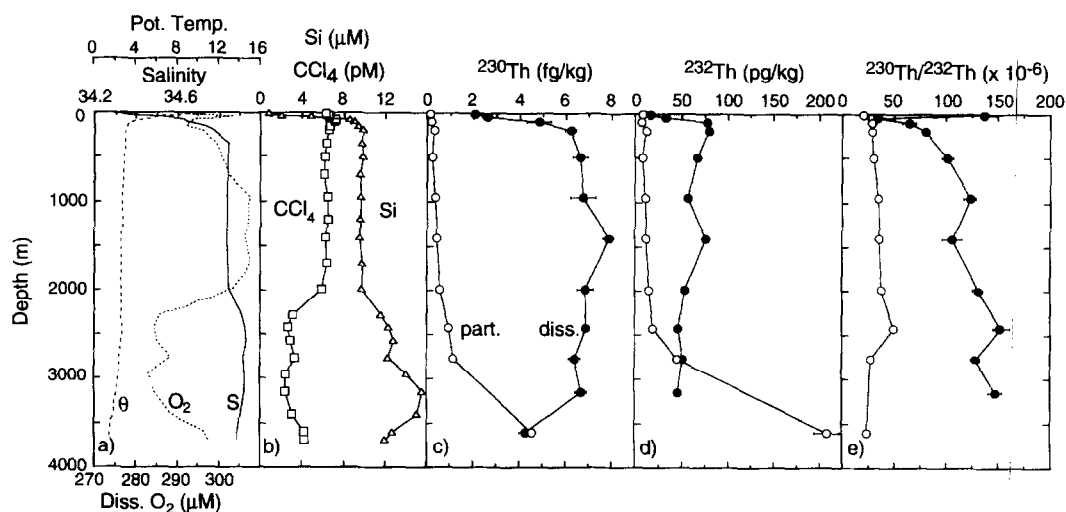


Fig. 2. Vertical profiles of dissolved oxygen, potential temperature, salinity, carbon tetrachloride, silicate, and dissolved and suspended particulate ^{230}Th , ^{232}Th and $^{230}\text{Th}/^{232}\text{Th}$ in the Labrador Sea.

which can be separated into upper (~ 400 – 950 m) and lower (~ 950 – 1900 m) LSW; upper LSW has lower oxygen and carbon tetrachloride concentrations compared to lower LSW. Below the LSW is the warmer and saltier Northeast Atlantic Deep Water (NEADW). This water mass extends from 2200 to 3300 m and shows a slight temperature maximum at ~ 2400 m and salinity maximum at ~ 3000 m. NEADW is older than the overlying LSW, as indicated by its lower carbon tetrachloride and dissolved oxygen concentrations and elevated Si values. The cold, low salinity Denmark Strait overflow water (DSOW) is evident as a deep boundary current within the bottom 100 m. The elevated carbon tetrachloride and dissolved oxygen concentrations and low Si values in this boundary flow indicate its more recent contact with the surface, and hence younger age, than the overlying NEADW.

3.2. ^{230}Th and ^{232}Th concentrations

^{230}Th and ^{232}Th results from the Labrador Sea, Denmark Strait, and Faeroe Bank Channel are listed in Table 1. Uncertainties in these results were calculated at the 2σ level and represent the maximum of run statistics (2σ mean) or counting statistics (2σ) fully propagated through corrections for blanks, multiplier dark noise, abundance sensitivity, and ^{230}Th in the ^{229}Th tracer.

Dissolved ^{230}Th and ^{232}Th concentrations range from 2.03 to 11.83 fg/kg (0.0929–0.541 dpm/1000 kg) and 14.75–78.97 pg/kg (0.00360–0.0193 dpm/1000 kg), respectively (Table 1). Particulate ^{230}Th and ^{232}Th concentrations in the Labrador Sea range from 0.13 to 4.54 fg/kg (0.00595–0.208 dpm/1000 kg) and 6.43–208.5 pg/kg (0.00157–0.0509 dpm/1000 kg). Particulate ^{230}Th represents 3–12% of the total throughout most of the water column and increases to 52% in the bottom waters. For ^{232}Th , the particulate fraction represents a greater fraction of the total, ranging from 31% at the surface (15 m) to 8–48% in the deep waters.

Particulate ^{232}Th and, to a lesser extent, ^{230}Th show a marked increase in the bottom 120 m. The likely explanation for the increase in particulate ^{232}Th and in the bottom waters is the presence of a nepheloid layer of resuspended sediments that characterize this boundary current. Elevated total dissolvable

Fe concentrations in the bottom waters have been found at this location [16,17]. Note that only an unfiltered water sample was available at this depth. Dissolved ^{230}Th was determined by the difference between the unfiltered and particulate samples. For ^{232}Th , the concentration in the unfiltered sample from the bottom waters is less than the measured particulate ^{232}Th (Table 1). Considering that particulate ^{232}Th probably accounts for most of the total ^{232}Th in this boundary current, the anomalously low total ^{232}Th may be an artifact of comparing a relatively large, integrated, particulate sample (~ 18 l filtered) with a small unfiltered sample (2 l).

Dissolved ^{230}Th concentrations in the Labrador deep waters are only slightly higher than in the Norwegian Sea [11] and deep eastern North Atlantic [6], whereas results from the western North Atlantic [7,12,17] are a factor of ~ 2 higher.

3.3. ^{230}Th and ^{232}Th distributions in the Labrador Sea

Within the upper 200 m of the Labrador Sea, vertical profiles of dissolved ^{230}Th and ^{232}Th are characterized by surface water minima (2.03 fg/kg, 15.1 pg/kg) and a sharp increase down to ~ 200 m (6.19 fg/kg and 78.9 pg/kg), respectively (Fig. 2c,d). As observed in the Norwegian Sea [11], dissolved ^{232}Th does not show a surface maximum due to external input (atmospheric or riverine), which is characteristic of other ocean regions [7,17,18]. Below ~ 200 m, the dissolved ^{230}Th profile is essentially invariant down to 3155 m, whereas dissolved ^{232}Th concentrations show a progressive decrease with depth. Particulate ^{230}Th and ^{232}Th concentrations are low in the surface waters and increase with depth and with proximity to the bottom. The boundary current in the bottom 120 m is characterized by low dissolved ^{230}Th (4.26 fg/kg) and elevated particulate ^{230}Th (4.54 fg/kg) and particulate ^{232}Th (208.5 pg/kg). The dissolved $^{230}\text{Th}/^{232}\text{Th}$ ratio shows a surface maximum (135×10^{-6}), a subsurface minimum (63.1×10^{-6}) and then increases with depth, whereas the particulate $^{230}\text{Th}/^{232}\text{Th}$ profile is essentially invariant throughout the water column (Fig. 2e).

Table 1
Salinity, potential temperature, and ^{230}Th and ^{232}Th results from the Labrador Sea, Denmark Strait and Faeroe Bank Channel, August, 1993

Depth (m)	Salinity	θ (°C)	^{230}Th (fg/kg)			^{232}Th (pg/kg)			$^{230}\text{Th}/^{232}\text{Th}$ ($\times 10^{-6}$)		
			Dissolved	Particulate	Total	Dissolved	Particulate	Total	Dissolved	Particulate	Total
Labrador Sea (IOC-93 Stn. 2; 54.50°N; 48.46°W; Depth 3713 m)											
15	34.297	10.73	2.03 ± 0.14	0.13 ± 0.02	2.16 ± 0.14	15.13 ± 0.78	6.92 ± 0.67	22.1 ± 1.0	135.0 ± 11.4	18.9 ± 3.4	98.6 ± 7.8
45	34.463	6.40	2.60 ± 0.21	–	–	32.06 ± 0.77	–	–	81.3 ± 6.8	–	–
100	34.606	3.50	4.82 ± 0.52	0.17 ± 0.02	5.00 ± 0.52	77.12 ± 1.20	6.43 ± 0.52	83.5 ± 1.3	63.1 ± 6.8	27.2 ± 4.3	60.3 ± 6.3
200	34.759	3.15	6.19 ± 0.22	0.29 ± 0.02	6.48 ± 0.22	78.97 ± 0.92	11.01 ± 0.92	90.0 ± 1.1	79.0 ± 3.0	26.9 ± 2.5	72.6 ± 2.7
500	34.840	3.07	6.64 ± 0.34	0.21 ± 0.01	6.84 ± 0.34	66.97 ± 1.31	7.47 ± 0.47	74.4 ± 1.4	99.9 ± 5.5	28.3 ± 2.6	92.7 ± 4.9
950	34.841	2.88	6.75 ± 0.33	0.35 ± 0.02	7.10 ± 0.33	55.81 ± 0.81	10.60 ± 0.47	66.4 ± 0.9	122.0 ± 6.2	33.7 ± 2.2	107.9 ± 5.3
1407	34.840	2.79	7.86 ± 0.56	0.40 ± 0.02	8.26 ± 0.56	75.74 ± 3.61	11.64 ± 0.71	87.3 ± 3.7	104.7 ± 8.9	34.7 ± 3.0	95.4 ± 7.6
1990	34.847	2.77	6.84 ± 0.23	0.53 ± 0.23	7.37 ± 0.23	53.36 ± 0.88	14.79 ± 0.61	68.2 ± 1.2	129.2 ± 4.8	36.1 ± 2.3	109.0 ± 3.8
2427	34.919	2.98	6.86 ± 0.35	0.91 ± 0.03	7.78 ± 0.35	45.82 ± 0.58	19.15 ± 0.64	64.7 ± 0.9	152.1 ± 8.0	48.1 ± 2.4	121.3 ± 5.7
2767	34.925	2.79	6.39 ± 0.15	1.13 ± 0.03	7.52 ± 0.16	50.68 ± 1.35	44.61 ± 0.63	95.3 ± 1.5	127.1 ± 4.61	25.6 ± 0.9	79.6 ± 2.1
3155	34.921	2.40	6.66 ± 0.25	–	–	45.89 ± 0.98	–	–	146.4 ± 6.3	–	–
3593	34.904	1.96	4.26 ± 0.28	4.54 ± 0.10	8.79 ± 0.26	–	208.5 ± 1.37	193.3 ± 1.02	45.9 ± 1.4	22.0 ± 0.5	45.9 ± 1.4
Denmark Strait (IOC-93, Stn. 12; 68.17°N, 22.67°W; Depth 1300 m)											
298	34.85	0.55	5.64 ± 0.37	–	–	58.34 ± 0.82	–	–	97.5 ± 6.5	–	–
Faeroe Bank Channel (IOC-93 Stn. 14; 61.44°N, 8.40°W; Depth 830 m)											
748	34.910	–0.33	2.75 ± 0.27	–	–	14.75 ± 2.38	–	–	188.0 ± 35.0	–	–
806	34.908	–0.41	11.83 ± 0.48	–	–	64.95 ± 1.56	–	–	183.8 ± 8.6	–	–

3.4. ^{230}Th and ^{232}Th in the overflow waters

The sample from 298 m in the northern Denmark Strait (Stn. 12) represents the end-member of the DSOW before it has descended into the near-bottom waters in the southern Denmark Strait at Stn. 7. This water mass has similar characteristics (salinity, freons, oxygen, and nutrients) to that observed within the bottom 125 m of the southern Denmark Strait at Stn. 7 [19]. The dissolved ^{230}Th concentration of 5.64 fg/kg at Stn. 12 (Table 1) is remarkably similar to values of 4.30–4.61 fg/kg in the core of recently formed DSOW at Stn. 7 [11]. For dissolved ^{232}Th , the concentration of 58.3 pg/kg at Stn. 12 is within the range of values of 24.4–142.5 pg/kg in the bottom ~ 100 m at Stn. 7 [11]. The low dissolved ^{230}Th signature of the DSOW at Stn. 12 and 7 is also evident in this dense water mass within the bottom ~ 100 m of the Labrador Sea (Table 1, Fig. 2c–e).

Samples collected at Stn. 14 are from the core of the Iceland–Scotland Sea overflow water (ISOW), which is derived from the Norwegian Sea at intermediate depths (~ 1000 m) and flows through the Faeroe Bank Channel into the Northeast Atlantic, forming a major part of the NEADW. Moran et al. [11] reported dissolved ^{230}Th and ^{232}Th concentrations of 5.81 fg/kg and 32.6 pg/kg, respectively, and a $^{230}\text{Th}/^{232}\text{Th}$ ratio of 180×10^{-6} at 872 m in the Norwegian Sea. These data are consistent with results for the ISOW of 2.75–11.83 fg/kg for ^{230}Th , 14.7–64.9 pg/kg for ^{232}Th , and $184\text{--}188 \times 10^{-6}$ for $^{230}\text{Th}/^{232}\text{Th}$ (Table 1).

An important result regarding the overflow waters is the remarkably constant ^{230}Th concentration in the Denmark Strait and Faeroe Bank Channel. With the exception of the bottom sample in the Faeroe Bank Channel, ^{230}Th values range from $\sim 3\text{--}5$ fg/kg (Table 1) [11]. Furthermore, ^{230}Th concentrations in the overflow waters increase by a factor of ~ 2 downstream in the deep Labrador Sea (excluding the bottom waters) and by a factor of ~ 4 in the deep waters off Cape Hatteras [7].

4. Discussion

4.1. Distribution of ^{230}Th in the deep waters

A key feature of the dissolved ^{230}Th distribution in the Labrador Sea is the relatively low and invari-

ant concentrations below ~ 500 m. It is clearly not possible to reproduce the ^{230}Th profile in the deep waters using a reversible scavenging model and a constant particle settling rate [8,20–22]. This lack of a constant increase in ^{230}Th with depth is also evident in the Norwegian Sea [11] and, to a lesser extent, in the Northwest Atlantic [7,17]. As discussed below, ^{230}Th distributions in these ocean basins are controlled by a combination of reversible scavenging and water mass ventilation.

4.2. A ^{230}Th scavenging–mixing model

According to the reversible thorium scavenging model [20], ignoring advection and diffusion, the concentration of dissolved ^{230}Th (C_d^{Th}) at depth z in the water column is given by:

$$C_d^{\text{Th}} = z \left(\frac{P_{\text{Th}}}{SK_d^{\text{Th}}SPM} \right) \quad (1)$$

where P_{Th} is the ^{230}Th production rate (0.56 fg/kg/yr; $= 2.6 \times 10^{-5}$ dpm/kg/yr); K_d^{Th} is the distribution coefficient for ^{230}Th ; SPM is the suspended particle concentration; and S is the particle settling speed, which represents the net effect of particle sinking, disaggregation and aggregation. This model predicts a linear increase in dissolved ^{230}Th with depth, such as observed in the western North Pacific [8].

In the case where the water mass residence time is similar to or less than the scavenging residence time of ^{230}Th in the deep ocean ($\sim 10\text{--}40$ yr; cf. [22]), the rate of ventilation becomes an important factor controlling ^{230}Th distributions. This is the case for the Labrador Sea, where the central gyre has a water mass age of approximately 8–10 yr (Rob Pickart, pers. commun.). Rutgers van der Loeff and Berger [9] developed a simple scavenging–mixing model that can be used to examine the role of ventilation on distributions of total ^{230}Th .

The model developed in this paper describes the evolution through time of a one-dimensional system, an ocean water column. The model considers reversible thorium scavenging [20] and water mass mixing, in a manner similar to mixing box models used to derive shelf-basin exchange times in the Arctic Ocean from chlorofluorocarbon [24] and ^{137}Cs

distributions [25]. An assumption made in applying the model to the Atlantic Ocean is that the system starts at time $t=0$ in the far North Atlantic and moves southward with time. Essentially, one can consider the model to represent the evolution through time of water in a pipe-flow reactor, where transport of material normal to the flow is permitted, to represent the effect of scavenging of radionuclides by sinking particles. The temporal evolution of vertical profiles of ^{230}Th reflects the net imbalance between production by U decay and removal by scavenging. Lateral exchange with water outside of the 1-D system is not permitted. The material balance for dissolved ^{230}Th at steady-state is:

$$\frac{dC_d^{\text{Th}}}{dt} = 0 = P_{\text{Th}} - \lambda C_d^{\text{Th}} + R - SK_d^{\text{Th}}SPM \left(\frac{\partial C_d^{\text{Th}}}{\partial z} \right) \quad (2)$$

where:

$$R = \frac{C_i^{\text{Th}} - C_d^{\text{Th}}(K_d^{\text{Th}}SPM + 1)}{T_w} \quad (3)$$

and C_i^{Th} is the initial concentration of total ^{230}Th in recently ventilated waters; that is, in newly formed NADW flowing over the sills in the Denmark Strait and Faeroe Bank Channel. The term T_w represents a water renewal time, or ventilation rate; for simplicity, T_w is defined as the time required to renew the

entire water column. Since $C_d^{\text{Th}} = 0$ at $z = 0$ and neglecting ^{230}Th decay we have:

$$C_d^{\text{Th}} = \frac{(C_i^{\text{Th}} + P_{\text{Th}}T_w)}{(K_d^{\text{Th}}SPM + 1)} \times \left[1 - \exp\left(-\frac{z(K_d^{\text{Th}}SPM + 1)}{SK_d^{\text{Th}}T_wSPM}\right) \right] \quad (4)$$

Eq. (4) is used to evaluate the large-scale effects of reversible scavenging and mixing on deep water distributions of dissolved ^{230}Th . Clearly, this simple 1-D model with lateral flushing of deep water from a northern source would not reproduce, for example, fine-scale features above the main thermocline. However, the primary purpose of using this model is to illustrate the effect of particle scavenging and water mass age on ^{230}Th in the deep Atlantic.

We first illustrate the effect of 'extreme' cases of scavenging and ventilation on deep water ^{230}Th distributions; in essence, a sensitivity analysis to illustrate the effect of scavenging and water mass age on ^{230}Th depth profiles. The model is evaluated for 'slow' and 'fast' particle removal of ^{230}Th by setting $S = 500$ m/yr and 1000 m/yr, respectively. These values span the range of the majority of particle settling speeds determined from oceanic ^{230}Th profiles [8,9,20–23]. In all cases, we use $K_d^{\text{Th}} = 1 \times 10^7$ ml/g and $SPM = 10$ $\mu\text{g}/\text{l}$, based on the average ^{230}Th $C_p/C_d = 0.1$ below 950 m (Table 1), which is similar to previous K_d^{Th} values [7,20,22]. The ^{230}Th

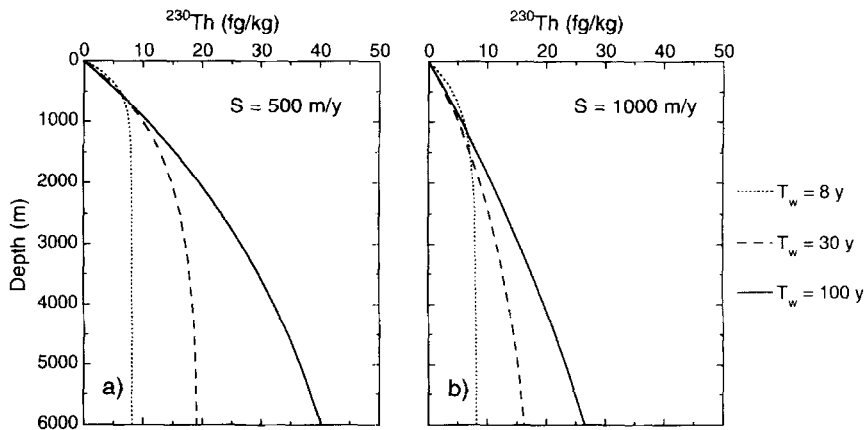


Fig. 3. Vertical profiles of dissolved ^{230}Th calculated using the scavenging–mixing model.

concentration in the over-flow waters indicates $C_i^{\text{Th}} = 4.5 \text{ fg/kg}$ (Table 1; [11]). Thus, the main adjustable parameter is T_w , which allows for direct examination of the effect of water mass age on deep water ^{230}Th distributions.

Profiles of ^{230}Th calculated using $S = 500 \text{ m/yr}$ and 1000 m/yr for various values of water mass age are presented in Fig. 3. The lower value of T_w was chosen to approximate the age of the Labrador Sea ($\sim 8\text{--}10 \text{ yr}$; Rob Pickart, pers. commun.). When $T_w = 100 \text{ yr}$, the ^{230}Th profile approaches an upper limit, which is the characteristic linear increase in ^{230}Th with depth according to Eq. (1). Clearly, for low values of S , the effect of ventilation rate on deep water ^{230}Th is substantial (Fig. 3a). For relatively young deep waters, ^{230}Th concentrations are low and invariant in the deep waters; when the ventilation rate is increased to 100 yr , ^{230}Th increases by up to $\sim 4\text{-fold}$ in the deep waters. Thus, for the case of slow particle removal, deep water ^{230}Th inventories are quite sensitive to changes in water mass age in the range $\sim 10\text{--}100 \text{ yr}$.

For the case of fast particle removal ($S = 1000 \text{ m/yr}$), ^{230}Th concentrations are considerably less sensitive to similar changes in water mass age (Fig. 3b). This is because ^{230}Th is more rapidly removed

via particle scavenging to the sediments. Even with a water mass age of $\sim 100 \text{ yr}$, deep water ^{230}Th concentrations do not increase to values presented for the case of slow particle removal (Fig. 3a). The net result is that deep water ^{230}Th concentrations remain relatively low for fast particle removal and are less sensitive to changes in ventilation rate.

4.3. Comparison of model results with ^{230}Th distributions in the Norwegian Sea and Atlantic

Fig. 4 presents a comparison between the model results and ^{230}Th profiles from: (1) the Norwegian Sea [11]; (2) Labrador Sea; (3) the North West Atlantic at the Bermuda Atlantic Time-series Station (BATS, [17]) and the Nares and Hatteras Abyssal Plains [7]; (4) the South Atlantic, north of the Polar Front [9]. Note that for the Norwegian Sea profile we set $C_i^{\text{Th}} = 0$ because this basin is likely ventilated with surface waters containing very low ^{230}Th [11].

The model results reproduce the large-scale feature of relatively low and constant ^{230}Th concentrations in northern Atlantic deep waters (Fig. 4). Using $S = 500 \text{ m/yr}$ and 1000 m/yr results in curves that generally bracket these data for short T_w values. This is because the major change in deep water

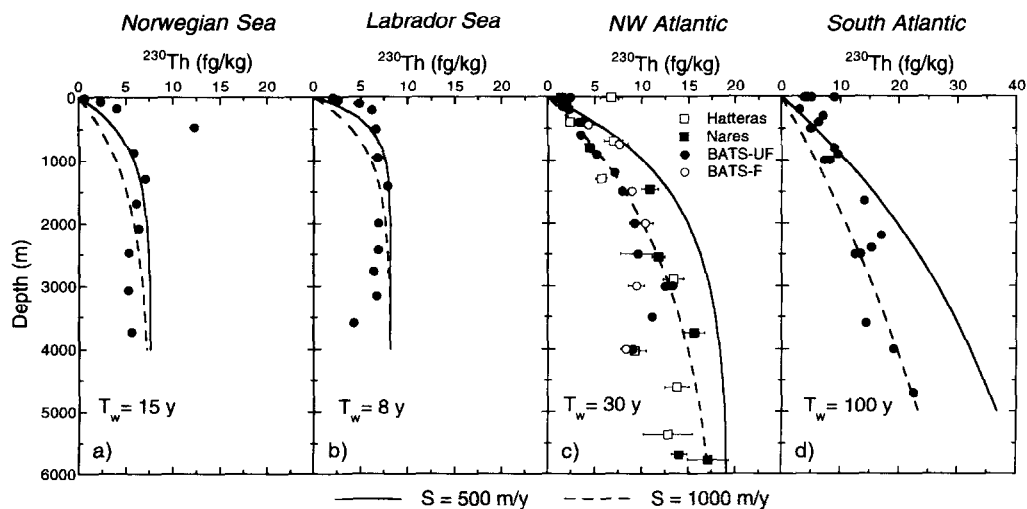


Fig. 4. Vertical profiles of dissolved ^{230}Th in the (a) Norwegian Sea (64.80°N , 6.20°W) [11]; (b) Labrador Sea (Stn. 2); (c) BATS ($31^\circ50'\text{N}$, $64^\circ10'\text{W}$) [17], Hatteras Abyssal Plain ($32^\circ46'$, $70^\circ47'\text{W}$), and Nares Abyssal Plain ($23^\circ11'\text{N}$, $63^\circ58'\text{W}$) [7]; (d) South Atlantic, north of the Antarctic Polar Front (Stn. 51, 55, 59, and 77) [9] (note change in concentration scale). Open symbols for BATS samples represent filtered ($< 0.2 \mu\text{m}$) ^{230}Th and closed symbols represent unfiltered samples. The scavenging–mixing model reproduces the major feature of relatively low and constant ^{230}Th evident in northern Atlantic deep waters.

^{230}Th occurs when T_w is increased and S is low (Fig. 3a). The ventilation age of 15 yr used to fit the Norwegian Sea profile is only slightly below the 20–30 yr range reported by Smethie et al. [26]. The Labrador Sea profile also is in good agreement with the model using $T_w = 8$ yr. The agreement between the model and ^{230}Th profiles from the Northwest Atlantic implies a deep water age of ~ 30 yr. By comparison, the average age of the entire deep western Atlantic is ~ 100 yr [27]. As a first approximation, it would seem reasonable to assume an age for the deep North Atlantic of ~ 50 yr, which is close to our deep water age at BATS. Finally, ^{230}Th results from the South Atlantic are in reasonable agreement with the model for $S = 1000$ m/yr, while the lower particle flux overestimates the ^{230}Th profile. Overall, the scavenging–mixing model reproduces the ^{230}Th profiles using reasonable deep water ages.

It is interesting to note the relatively low ^{230}Th concentration in the bottom waters of the Labrador Sea compared to the model profile (Fig. 4b). This bottom water ^{230}Th sample is from the core of the DSOW and is similar to the mean value of ~ 4.5 fg/kg measured in the overflow waters (Table 1; [11]). It is therefore expected that the ^{230}Th content of the Labrador Sea bottom waters would be lower, due to their more recent contact with the DSOW and hence younger age, than the deep/intermediate waters.

The implication of these results is that the deep water inventory of ^{230}Th in the North Atlantic is sensitive to changes in ventilation rate on a time-scale of ~ 10 – 100 yr. If NADW production decreased in the past, for example during the Younger Dryas or Heinrich events, and particle flux remained relatively constant (or decreased), then deep water ^{230}Th in the North Atlantic would be expected to increase substantially over a period of only ~ 100 yr (Fig. 3a). This effect should be pronounced in the Labrador Sea, where deep water ^{230}Th concentrations are a factor of ~ 2 lower than near Bermuda. Alternatively, if the particle flux in this region was higher during glacial times, deep water ^{230}Th would not change markedly in response to a decrease in NADW production (Fig. 3b). Excess sedimentary ^{230}Th and $^{231}\text{Pa}/^{230}\text{Th}$ ratios [1] in cores from the Labrador Sea may provide information on the timing of abrupt changes in NADW production in the past.

5. Conclusions

Advection is important in controlling the distribution of the particle-reactive tracer ^{230}Th in the deep ocean. This is particularly evident in ocean basins with short deep water residence times ($\sim < 100$ yr), such as the north Atlantic and possibly the Arctic. Conversely, advective transport is expected to be less important for ^{230}Th in older deep waters, such as in the north Pacific. Thus, the large-scale feature of relatively low and invariant ^{230}Th in the deep north Atlantic can be explained using a reversible scavenging model that includes the effect of ventilation. Advective transport must also be important in the redistribution of other long-lived radionuclides, such as ^{231}Pa , ^{26}Al and ^{10}Be in the deep Atlantic.

Acknowledgements

We wish to acknowledge the support of the IOC, the Canadian government for use of the CSS *Hudson*, the Captain and crew of the CSS *Hudson*, Chief Scientist P.A. Yeats and the NSF for sponsoring the IOC cruises. We are grateful to R.F. Anderson, M.P. Bacon, W.S. Broecker, H.N. Edmonds and two anonymous reviewers for thorough and critical reviews. Lynn Hettinger corrected an error in our original calculations. This work was funded by NSF grants OCE-9408945 to SBM and OCE-9203150, OCE-9402693, and EAR-9406183 to RLE. [MK]

References

- [1] E.-F. Yu, R. Francois, M.P. Bacon, Similar rates of modern and last-glacial ocean thermohaline circulation inferred from radiochemical data, *Nature* 379 (1996) 689–694.
- [2] H.S. Yang, Y. Nozaki, H. Sakai, A. Masuda, The distribution of ^{230}Th and ^{231}Pa in the deep-sea surface sediments of the Pacific Ocean, *Geochim. Cosmochim. Acta* 50 (1986) 81–99.
- [3] M.P. Bacon, Tracers of chemical scavenging in the ocean: boundary effects and large-scale chemical fractionation, *Philos. Trans. R. Soc. London, Ser. A* 325 (1988) 147–160.
- [4] R.F. Anderson, Y. Lao, W.S. Broecker, S.E. Trumbore, H.J. Hofmann, W. Wolfli, Boundary scavenging in the Pacific Ocean: a comparison of ^{10}Be and ^{231}Pa , *Earth Planet. Sci. Lett.* 96 (1990) 287–304.
- [5] Y. Lao, R.F. Anderson, W.S. Broecker, Boundary scavenging and deep sea sediment dating: constraints from excess ^{230}Th and ^{231}Pa , *Paleoceanography* 7 (1992) 783–798.

- [6] A. Mangini, R.M. Key, A ^{230}Th profile in the Atlantic Ocean, *Earth Planet. Sci. Lett.* 62 (1983) 377–384.
- [7] J.K. Cochran, H.D. Livingston, D.J. Hirschberg, L.D. Suprenant, Natural and anthropogenic radionuclide distributions in the northwest Atlantic Ocean, *Earth Planet. Sci. Lett.* 84 (1987) 135–152.
- [8] Y. Nozaki, Y. Horibe, H. Tsubota, The water column distributions of thorium isotopes in the western North Pacific, *Earth Planet. Sci. Lett.* 54 (1981) 203–216.
- [9] M.M. Rutgers van der Loeff, G.W. Berger, Scavenging of ^{230}Th and ^{231}Pa near the Antarctic Polar Front in the South Atlantic, *Deep-Sea Res.* 40 (2) (1993) 339–357.
- [10] E.-F. Yu, Variations in the particulate flux of ^{230}Th and ^{231}Pa and paleoceanographic applications of the $^{231}\text{Pa}/^{230}\text{Th}$ ratio, Ph.D. Thesis, MIT/WHOI, WHOI-94-21, 1994.
- [11] S.B. Moran, J.A. Hoff, K.O. Buesseler, R.L. Edwards, High precision ^{230}Th and ^{232}Th in the Norwegian Sea and Denmark Strait by thermal ionization mass spectrometry, *Geophys. Res. Lett.* 22 (1995) 2589–2592.
- [12] J.H. Chen, R.L. Edwards, G.J. Wasserburg, ^{238}U , ^{234}U and ^{232}Th in seawater, *Earth Planet. Sci. Lett.* 80 (1986) 241–251.
- [13] R.L. Edwards, J.H. Chen, G.J. Wasserburg, ^{238}U – ^{234}U – ^{230}Th – ^{232}Th systematics and the precise measurement of time over the past 500,000 years, *Earth Planet. Sci. Lett.* 81 (1986) 175–192.
- [14] H. Cheng, R.L. Edwards, S.J. Goldstein, Pa-231 dating of carbonates using TIMS techniques, *EOS Trans. Am. Geophys. Union* 77 (1996) S168.
- [15] D.W. Eggiman, P.R. Betzer, Decomposition and analysis of refractory oceanic suspended materials, *Anal. Chem.* 48 (1976) 886–890.
- [16] W.M. Landing, R.T. Powell, D. Whitney King, Distributions of dissolved and particulate iron in the Atlantic Ocean: results from the 1990 and 1993 IOC Trace Metals Baseline Expedition, *EOS Trans. Am. Geophys. Union* 75 (44) (1994) 324.
- [17] J.A. Hoff, R.L. Edwards, K.O. Buesseler, R.A. Belostock, S.B. Moran, TIMS measurements of ^{230}Th and ^{232}Th in liter-sized samples of seawater from the Northwest Atlantic Ocean, *Geochim. Cosmochim. Acta* (1996), in prep.
- [18] C.-H. Huh, W.S. Moore, D.C. Kadko, Oceanic ^{232}Th : a reconnaissance and implications of global distribution from manganese nodules, *Geochim. Cosmochim. Acta* 53 (1989) 1357–1366.
- [19] P.A. Yeats, C.I. Measures, The hydrographic setting of the second IOC contaminants baseline cruise, *Mar. Chem.* (1996) submitted.
- [20] M.P. Bacon, R.F. Anderson, Distribution of thorium isotopes between dissolved and particulate forms in the deep sea, *J. Geophys. Res.* 87 (1982) 2045–2056.
- [21] Y. Nozaki, Y. Horibe, Alpha-emitting thorium isotopes in northwest Pacific deep waters, *Earth Planet. Sci. Lett.* 65 (1983) 39–50.
- [22] Y. Nozaki, H.S. Yang, M. Yamada, Scavenging of thorium in the ocean, *J. Geophys. Res.* 92 (1987) 772–778.
- [23] J.C. Scholten, M.M. Rutgers van der Loeff, A. Michel, Distribution of ^{230}Th and ^{231}Pa in the water column in relation to the ventilation of the deep Arctic basins, *Deep-Sea Res.* 42 (1995) 1519–1531.
- [24] D.W.R. Wallace, R.M. Moore, Vertical profiles of CCl_3F (F-11) and CClF_2 (F-12) in the Central Arctic Ocean Basin, *J. Geophys. Res.* 90 (C1) (1985) 1155–1166.
- [25] J.N. Smith, K.M. Ellis, Radionuclide tracer profiles at the CESAR Ice Station and Canadian Ice Island in the western Arctic Ocean, *Deep-Sea Res.* 42 (6) (1995) 1449–1470.
- [26] W.M.Jr. Smethie, H.G. Ostlund, H.H. Loosli, Ventilation of the deep Greenland and Norwegian seas: evidence from krypton-85, tritium, carbon-14, and argon-39, *Deep-Sea Res.* 33 (5) (1986) 657–703.
- [27] W.S. Broecker, T.-H. Peng, *Tracers in the Sea*, Lamont-Doherty Geol. Observ., Columbia Univ., 1982, pp. 690.